

# Image-based Multimodal Models as Intruders: Transferable Multimodal Attacks on Video-based MLLMs

Linhao Huang<sup>1,2\*</sup> Xue Jiang<sup>2,3\*</sup> Zhiqiang Wang<sup>4\*</sup> Wentao Mo<sup>1,2</sup>  
Xi Xiao<sup>1†</sup> Bo Han<sup>3</sup> Yongjie Yin<sup>5</sup> Feng Zheng<sup>2†</sup>

<sup>1</sup>Tsinghua Shenzhen International Graduate School, Tsinghua University

<sup>2</sup>Southern University of Science and Technology <sup>3</sup>TMLR Group, Hong Kong Baptist University

<sup>4</sup>Hong Kong University of Science and Technology <sup>5</sup>China Electronics Corporation

{hlh23, mow10}@mails.tsinghua.edu.cn

{csxjiang, bhanml}@comp.hkbu.edu.hk,

zwangmk@connect.ust.hk, xiaox@sz.tsinghua.edu.cn

yinyongjie@mail.bnu.edu.cn, f.zheng@ieee.org

## Abstract

Video-based multimodal large language models (V-MLLMs) have shown vulnerability to adversarial examples in video-text multimodal tasks. However, the transferability of adversarial videos to unseen models—a common and practical real-world scenario—remains unexplored. In this paper, we pioneer an investigation into the transferability of adversarial video samples across V-MLLMs. We find that existing adversarial attack methods face significant limitations when applied in black-box settings for V-MLLMs, which we attribute to the following shortcomings: (1) lacking generalization in perturbing video features, (2) focusing only on sparse key-frames, and (3) failing to integrate multimodal information. To address these limitations and deepen the understanding of V-MLLM vulnerabilities in black-box scenarios, we introduce the Image-to-Video MLLM (I2V-MLLM) attack. In I2V-MLLM, we utilize an image-based multimodal model (IMM) as a surrogate model to craft adversarial video samples. Multimodal interactions and temporal information are integrated to disrupt video representations within the latent space, improving adversarial transferability. In addition, a perturbation propagation technique is introduced to handle different unknown frame sampling strategies. Experimental results demonstrate that our method can generate adversarial examples that exhibit strong transferability across different V-MLLMs on multiple video-text multimodal tasks. Compared to white-box attacks on these models, our black-box attacks (using BLIP-2 as surrogate model) achieve competitive performance, with

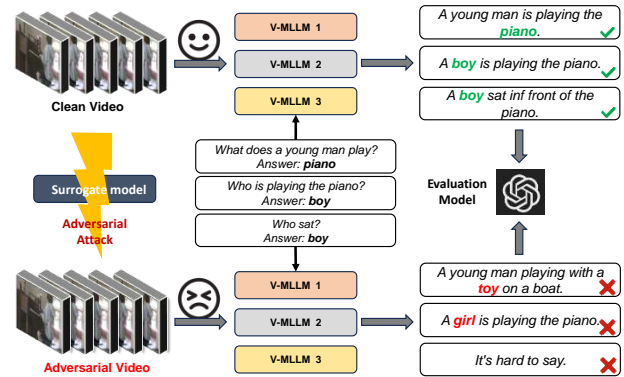


Figure 1. An example of transferable adversarial attack on different target V-MLLMs for VideoQA task.

average attack success rates of 55.48% on MSVD-QA and 58.26% on MSRVTT-QA for VideoQA tasks, respectively. Our code will be released upon acceptance.

## 1. Introduction

Recent work has shown that video-based multimodal large language models (V-MLLMs) are vulnerable to adversarial video samples [21], even though they have achieved remarkable performance on a wide range of video-text multimodal tasks [9, 18, 22, 24, 29, 42]. Existing work primarily focuses on white-box attacks, where information about the target model is accessible. However, the transferability of adversarial video samples across V-MLLMs remains unexplored, which is a more common and practical setting in real-world scenarios. It is still uncertain whether the adver-

\*Equal contribution.

†Corresponding author.

arial videos generated on the source model can effectively attack other target models, posing significant security risks to the deployment of V-MLLMs in real-world applications.

In this paper, we pioneer an investigation into the transferability of adversarial video samples across V-MLLMs. Through detailed analysis in Sec. 3.2, we think previous methods have these shortcomings: (1) lacking generalization in perturbing video features, (2) focusing only on sparse key-frames, and (3) failing to integrate multimodal information. FMM attack [21] is the first proposed white-box attack method targeting V-MLLMs. It utilizes flow-based temporal mask to select key-frames and applies perturbations to these frames. FMM attack performs well in the white-box setting but has limited transferability in the black-box setting. FMM attack heavily relies on the video features, which causes the generated perturbations to overfit to the video features extracted by the surrogate model, thereby reducing their generalizability. Additionally, since FMM attack applies perturbations only to key-frames, it cannot ensure that all frames sampled by the target model are perturbed. Taking low-level image features into account can help with improving transferability of adversarial samples. Previous image-to-video cross-modal attacks [19, 37, 39] demonstrate the possibility of using image models as surrogates to attack video models in the black-box setting. However, these traditional attack methods typically focus on the video classification tasks with vision-only models, failing to integrate multimodal information.

To address these limitations, we propose a highly transferable attack method, named as Image To Video MLLM (I2V-MLLM) attack (see Fig. 2). In I2V-MLLM, we utilize an image-based multimodal model (IMM) as a surrogate model to craft adversarial video samples without accessing the internals of target V-MLLMs. Specifically, we extract key-frames from videos and send them into an IMM to obtain adversarial perturbations. Multimodal interactions and temporal information are integrated to disrupt video representations within the latent space, improving adversarial transferability. In addition, a perturbation propagation technique is introduced to handle different unknown frame sampling strategies used by V-MLLMs.

We conduct various experiments on three well-established datasets, MSVD-QA [41], MSRVT-QA [41], and ActivityNet-200 [15] to evaluate the performance of our proposed I2V-MLLM attack in multiple video-text multimodal tasks. The experimental results demonstrate that our method can generate adversarial videos with strong transferability across different V-MLLMs (Chat-Univi [18], LLaVA-Next-Video [44], VideoChat [22], Video-LLaMA [42]), and achieve competitive performance with white-box attacks against V-MLLMs. Our main contributions are summarized as follows:

- We explore the transferable adversarial attack on four dif-

ferent V-MLLMs and analyze the reasons for the low transferability when using existing methods to generate adversarial video samples (see Sec. 3.2). To the best of our knowledge, this is the first work to explore black-box attacks on V-MLLMs.

- We propose a highly transferable attack method, named I2V-MLLM, for V-MLLMs using IMM to generate adversarial video samples (see Sec. 3.3). The adversarial videos generated by this method can effectively disrupt different V-MLLMs, significantly degrading their performance on multiple video-text multimodal tasks.
- We conduct extensive experiments on four different V-MLLMs using MSVD-QA, MSRVT-QA, and ActivityNet-200 (see Sec. 4.2 and Sec. 4.3). The results demonstrate that our proposed attack method has strong transferability across V-MLLMs.

## 2. Related work

### 2.1. Multimodal large language models

MLLMs typically consist of a vision model, a pretrained LLM, and a projector that translates visual information into textual representations that the LLM can process. Currently, MLLMs can be categorized into image-based and video-based types. Image-based MLLMs [1–3, 9, 16, 26, 46] are designed to handle image-text inputs. They excel in tasks such as visual question answering, image captioning, and more. V-MLLMs extend the capabilities of image-based MLLMs by incorporating temporal modules that allow them to understand and process video input. This enables them to perform tasks like video question answering (VideoQA), spatio-temporal localization, and video captioning. For example, Chat-UniVi [18] extracts specific frames from videos and utilizes DPC-KNN [12] to group these frames into distinct events, Video-LLaMA [42] employs sequential encoding to capture temporal relationships among video frames, VideoChatGPT [29] applies temporal pooling to video features to extract temporal information. These methods equip the models with the capability to capture and interpret temporal dynamics, thus enabling a more comprehensive understanding of video content.

### 2.2. Adversarial attacks on MLLMs

Despite the impressive performance, MLLMs are highly susceptible to adversarial attacks [4, 8, 27, 28, 36, 43, 45]. For image-based MLLMs, several studies have assessed their vulnerabilities to adversarial attacks. Fu et al. [13] introduce Trojan-like images that force the target models to invoke malicious external tools or APIs specified by the attacker. Dong et al. [11] utilize open-source MLLMs to generate transferable adversarial examples capable of attacking closed-source commercial models like Bard [14], Bing Chat [31], and GPT-4V [33], thereby showing high transfer-

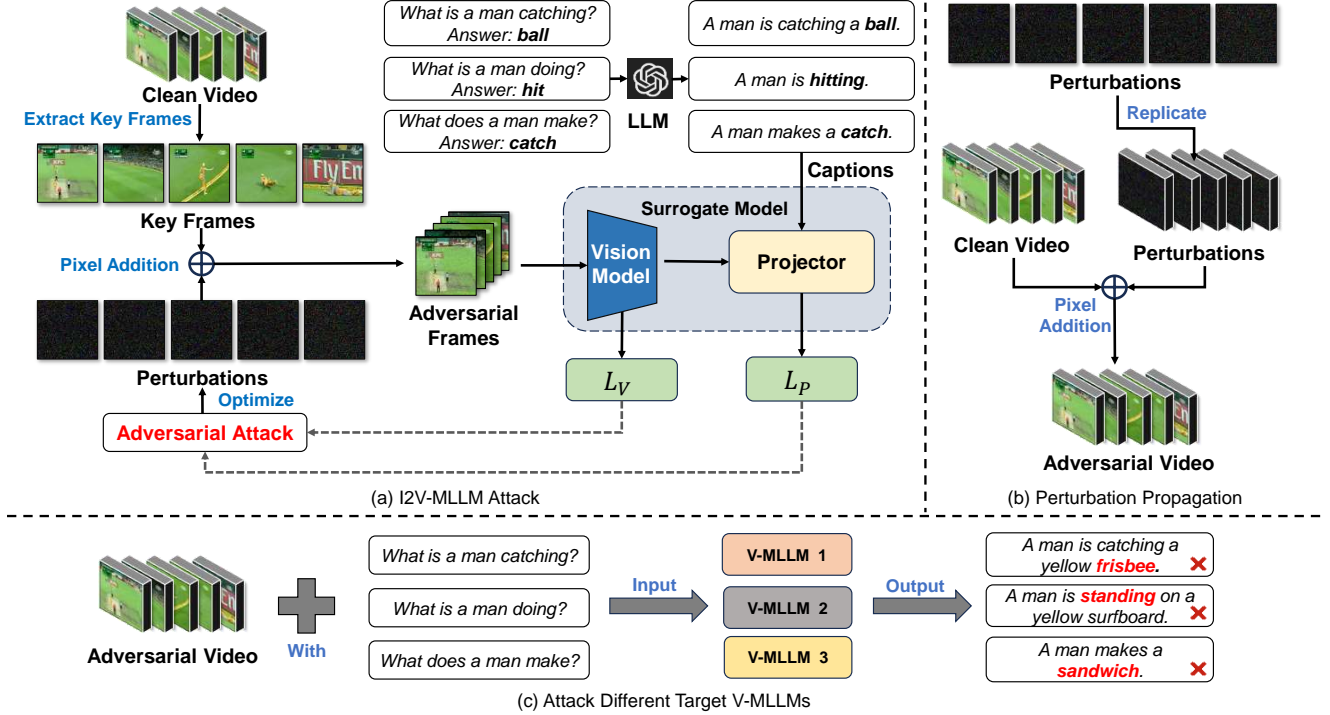


Figure 2. The overview of our proposed I2V-MLLM attack.

ability of adversarial examples across MLLMs. While extensive studies have explored adversarial attacks on image-based MLLMs, there has been little exploration in the domain of V-MLLMs. Li et al. [21] propose a flow-based adversarial attack strategy for white-box attacks on V-MLLMs. However, in real-world scenarios, the internal architectures and parameters of V-MLLMs are usually inaccessible to users. To address this, we focus on exploring methods for conducting adversarial attacks on V-MLLMs in a black-box setting.

### 2.3. Adversarial attack on video models

Current video models have diverse applications, including autonomous vehicles, video verification, security, and other fields. However, these models remain vulnerable to adversarial attacks [6, 17, 23, 38, 40]. For example, Universal 3D perturbations (U3D) [40] deceive video classifiers by generating a universal perturbation for all input videos, while StyleFool [5] introduces an unrestricted perturbation to attack video classification systems through style transfer. Recent studies also explore cross-modal attack methods from image models to video models [19, 37, 39], yielding promising results. However, these attacks primarily target video classification tasks, which do not account for interactions between visual and textual modalities. In contrast, V-MLLMs integrate both visual and textual information, rendering these methods unsuitable for such models. To address this limitation, our method incorporates multimodal

interactions when crafting adversarial video samples, aligning with the operational principles of V-MLLMs.

## 3. Methodology

### 3.1. Preliminary

Given a video sample  $V \in \mathcal{V}$  with  $M$  associated QA pairs  $\{(q_m, a_m)\}_{m=1}^M$ , where  $q_m$  is the  $m$ -th question and  $a_m$  is the corresponding answer. Let  $F$  denote the IMM (e.g., BLIP-2 [20], MiniGPT-4 [46]) and  $G$  denote the V-MLLM (e.g., Video-LLaMA [42], Chat-UniVi [18]). We use  $G(V, q)$  to denote the answer generated by the V-MLLM for the given video  $V$  and question  $q$ . The goal of our proposed attack is to generate an adversarial example  $V_{adv} = V + \delta'$  using  $F$ , which can cause  $G$  to produce an answer  $G(V_{adv}, q_i)$  that differs significantly from the correct answer  $a_i$ , without accessing the parameters or structure of  $G$ , where  $\delta'$  denotes the adversarial perturbations specifically tailored for  $V$ . To ensure that the adversarial perturbation  $\delta'$  is imperceptible, we restrict it by  $\|\delta'\|_\infty \leq \epsilon$ , where  $\|\cdot\|_\infty$  denotes the  $L_\infty$  norm, and  $\epsilon$  is a constant for the norm constraint. We utilize the evaluation model  $E$  (i.e., GPT-4o-mini [32]) to assess whether the generated answer aligns with the reference answer. We aim to find adversarial perturbations that minimize the number of correct responses, formulated as follows:

Attack	Target Model			
	Chat-UniVi	LLaVA-NeXT-Video	VideoChat	Video-LLaMA
<b>FMM</b>	8.11	15.38	14.62*	20.74
<b>Vanilla</b>	8.22	15.86	35.03*	19.81
<b>I2V</b>	25.17	27.39	27.13	30.51
<b>FMM w/ Prop.</b>	14.54	28.31	14.62*	27.38
<b>Vanilla w/ Prop.</b>	13.59	23.06	35.03*	27.98
<b>I2V-MLLM</b>	<b>43.39</b>	<b>40.54</b>	<b>63.09</b>	<b>74.91</b>

Table 1. Attack success rates (ASR, %) on the MSVD-QA validation set for VideoQA tasks. **FMM** and **I2V** denote attack methods from [21] and [39], respectively. **Vanilla** attack applies full perturbations on all key-frames sampled by V-MLLMs. **Prop.** denotes perturbation propagation. \* indicates white-box attacks. A higher ASR indicates better adversarial transferability.

$$\operatorname{argmin}_{\delta'} \frac{1}{M} \sum_{i=1}^M E(G(V + \delta', q_i), a_i), \text{ s.t. } \|\delta'\|_{\infty} \leq \epsilon, \quad (1)$$

where  $E(\cdot, \cdot)$  is the evaluation model’s judgment function, which outputs 1 if they match, and 0 otherwise.

### 3.2. Motivation

To explore the transferability of adversarial videos across V-MLLMs, we first conduct an investigation of existing attack methods. Based on the experimental results (in Tab. 1), we attribute their poor transferability to the following limitations: (1) focusing only on sparse key-frames, (2) lacking generalization in perturbing video features, and (3) failing to integrate multimodal information.

**Focusing only on sparse key-frames.** The FMM attack exhibits limited transferability in the black-box setting due to differences in key-frame selection between the attack method and V-MLLMs. To address this, we first modify the FMM attack by replacing the sparse spatial perturbation with full perturbation on the key-frames sampled by V-MLLMs, which we call the Vanilla attack. While this adjustment improves white-box performance, the transferability still remains constrained. To further enhance transferability, we propagate perturbations from key-frames across the entire video, leading to improved transferability, as shown in rows 1, 2, 4, and 5 of Tab. 1.

**Lacking generalization in perturbing video features.** Adversarial perturbations generated based on certain V-MLLM can overfit to specific video module, limiting their generalization to other V-MLLMs. To improve transferability, we focus on lower-level image features. The I2V attack [39], which perturbs each video frame to disrupt image features, demonstrates improved transferability when using image models as surrogates to craft adversarial video samples, as shown in rows 3, 4, and 5 of Tab. 1.

**Failing to integrate multimodal information.** The I2V attack shows a limited improvement in transferability, as it was originally designed for video classification and does

not account for the multimodal interactions, which is essential for V-MLLMs. Therefore, we propose using an image-based multimodal model as a surrogate, integrating multimodal interaction information into the process of generating adversarial video samples, which leads to a significant improvement in transferability, as demonstrated in rows 3 and 6 of Tab. 1.

In summary, we propose using IMM as surrogates to generate adversarial video samples that incorporate multimodal interactions. In addition, we introduce a perturbation propagation technique to handle different unknown frame sampling strategies. The I2V-MLLM results in Tab. 1 demonstrate the strong transferability of our method across different V-MLLMs. More discussions can be found in Appendix A. The following sections describe our proposed attack in detail.

### 3.3. I2V-MLLM Attack

The proposed I2V-MLLM attack utilizes an IMM to produce adversarial video samples, targeting image-to-video cross-modal black-box attacks on V-MLLMs with significant transferability. By manipulating the intermediate features of vision models and projectors of IMM, our approach generates adversarial video samples that interfere with the intermediate features of black-box V-MLLMs. The I2V-MLLM algorithm is illustrated in Appendix C, consists of three components: vision model attack, projector attack, and perturbation propagation.

#### 3.3.1. Vision Model Attack

To enhance generalization in perturbing video features, I2V-MLLM disrupts both image features and spatiotemporal information extracted by the vision model. We first split the video  $V$  into  $K$  clips:  $V = \{v^1, v^2, \dots, v^K\}$ , where  $K = \text{total number of frames} \times \text{key-frame ratio } \beta$ . We select the first frame  $x^k$  from each clip  $v^k$  as the key-frame, resulting in  $K$  key-frames,  $X = \{x^1, x^2, \dots, x^K\}$ , each capturing the essential information of their respective clips. Following [29], we extract spatiotemporal representations of  $X$  using the vision model. This model independently encodes the  $K$  frames, producing frame-level embeddings  $F_V(X) \in \mathbb{R}^{K \times N \times D_1}$ , where  $F_V(\cdot)$  denotes the encoder of the vision model,  $N$  is the number of patches per frame, and  $D_1$  is the dimension of the embeddings. Frame-level embeddings are average-pooled along the temporal dimension to obtain a video-level temporal representation  $F_V^t(X) \in \mathbb{R}^{N \times D_1}$ , which implicitly incorporates temporal learning through the aggregation of  $K$  frames. Similarly, the frame-level embeddings are average-pooled along the spatial dimension to obtain a video-level spatial representation  $F_V^s(X) \in \mathbb{R}^{K \times D_1}$ , which incorporate the spatial information of  $K$  frames. The temporal and spatial features are concatenated to obtain the original video-level features

$F_V^{ts}(X) = [F_V^t(X), F_V^s(X)] \in \mathbb{R}^{(N+K) \times D_1}$ . For the adversarial input  $X_{adv} = \{x^1 + \delta^1, x^2 + \delta^2, \dots, x^K + \delta^K\}$ , we can similarly obtain the adversarial video-level features  $F_V^{ts}(X_{adv})$ . To disrupt the video-level features, I2V-MLLM optimizes the adversarial perturbations by minimizing the cosine similarity between the original and the adversarial video features:

$$\mathcal{L}_V = \sum_{i=1}^{N+K} \frac{\text{Cos}(F_V^{ts}(X)_i, F_V^{ts}(X_{adv})_i)}{N+K}, \quad (2)$$

where  $F_V^{ts}(X)_i$  and  $F_V^{ts}(X_{adv})_i$  represent the  $i$ -th elements in the video-level features of the original and the adversarial video frames, respectively.

### 3.3.2. Projector Attack

To further disrupt V-MLLMs’ capacity for video-text multimodal tasks, I2V-MLLM interferes with the intermediate feature of the projector (e.g. Q-Former [20]), which plays an essential role in aligning visual and textual representations. We feed the projector with the original frame-level embeddings  $F_V(X)$ , the adversarial frame-level embeddings  $F_V(X_{adv})$  from the vision model, and the caption set  $T = \{t_1, t_2, \dots, t_M\}$ . After multimodal alignment, they are transformed into the original visual features  $F_P^v(X) \in \mathbb{R}^{N_1 \times D_2}$ , the adversarial visual features  $F_P^v(X_{adv}) \in \mathbb{R}^{N_1 \times D_2}$ , and the textual features  $F_P^t(T) \in \mathbb{R}^{N_2 \times D_2}$ . Here,  $N_1$  and  $N_2$  represent the number of visual features and the textual features, respectively. And  $D_2$  denotes the dimension of these features. The captions are complete sentences generated based on the question  $q$  and the answer  $a$  using GPT-4o-mini [32]. For example, given the question  $q$ : ‘What is the man doing?’ and the answer  $a$ : ‘eat’, the corresponding caption  $t$  would be: ‘The man is eating.’ To perturb the image features aligned with the text, I2V-MLLM optimizes the adversarial perturbations by minimizing the cosine similarity between the original and the adversarial visual features:

$$\mathcal{L}_{P_v} = \sum_{n_1=1}^{N_1} \frac{\text{Cos}(F_P^v(X)_{n_1}, F_P^v(X_{adv})_{n_1})}{N_1}, \quad (3)$$

where  $F_P^v(X)_{n_1}$  and  $F_P^v(X_{adv})_{n_1}$  are the  $n_1$ -th visual feature of the original and the adversarial video frames, respectively. To disrupt multimodal interactions between adversarial frames and text, I2V-MLLM optimizes the adversarial perturbations by minimizing the cosine similarity between the adversarial visual features and the textual features:

$$\mathcal{L}_{P_{v2t}} = \sum_{n_1=1}^{N_1} \sum_{n_2=1}^{N_2} \frac{\text{Cos}(F_P^v(X_{adv})_{n_1}, F_P^t(T)_{n_2})}{N_1 N_2}, \quad (4)$$

where  $F_P^t(T)_{n_2}$  is the  $n_2$ -th textual feature of  $T$ . The total loss function for projector is

$$\mathcal{L}_P = \mathcal{L}_{P_v} + \mathcal{L}_{P_{v2t}}. \quad (5)$$

### 3.3.3. Optimization and Perturbation Propagation

To maximize the efficacy of the adversarial attack, we combine the losses  $\mathcal{L}_V$  and  $\mathcal{L}_P$  into a unified objective. This combined loss ensures that both the vision model and the projector’s intermediate features are significantly perturbed. The unified loss is formulated as:

$$\mathcal{L}_{total} = \lambda_1 \mathcal{L}_V + \lambda_2 \mathcal{L}_P, \quad (6)$$

where  $\lambda_1$  and  $\lambda_2$  correspond to the two loss weights, which aim to balance them during the optimization.

We optimize  $\delta_k$  according to the following expression:

$$\delta^k = \arg \min_{\delta^k} (\mathcal{L}_{total}), s.t. \|\delta^k\|_\infty \leq \epsilon, k = 1, 2, \dots, K. \quad (7)$$

Finally, we replicate  $\delta^k$  to match the length of its corresponding video clip  $v^k$ , resulting in  $\delta'^k$ . We then construct the adversarial video by adding these perturbed clips to the original clips:  $V_{adv} = V + \delta' = \{v^1 + \delta'^1, v^2 + \delta'^2, \dots, v^K + \delta'^K\}$ .

## 4. Experiment

### 4.1. Experimental setting

In this section, we present the experimental setting, including datasets, models, attack setting and metrics.

**Datasets and models.** Referring to the quantitative benchmarking framework proposed in [29], we evaluate our I2V-MLLM attack on VideoQA tasks using the validation set of MSRVT-QA [41] and MSVD-QA [41], and on video understanding tasks using a subset of ActivityNet-200 [15]. We perform the proposed method on three IMMs: BLIP-2 [20], InstructBLIP [9] and MiniGPT-4 [46]. Our method is evaluated on four different V-MLLMs: Chat-UniVi [18], LLaVA-NeXT-Video [44], VideoChat [22], and Video-LLaMA [42], each with a Vicuna-7B [7] as the LLM.

**Attack setting.** In I2V-MLLM, we employ the projected gradient descent (PGD) [30] with a perturbation bound of  $\epsilon = 16$ , an iteration number of  $I = 50$ , and a step size of  $\alpha = 1$  for the attack process. The parameters  $\lambda_1$  and  $\lambda_2$  are both set to 1, and the key-frame ratio  $\beta$  is set to 30%. I2V attack, utilizing CLIP-L/14 [34] as the surrogate model, applies tailored perturbations to each frame of the video. For a fair comparison, the PGD parameters ( $\epsilon = 16$ ,  $I = 50$  and  $\alpha = 1$ ) in FMM, Vanilla, and I2V attacks maintain the same for our method. Additionally, in the FMM setup, the key-frame ratio  $\beta$  is also set to 30%. All the experiments are conducted on a single NVIDIA-A6000 GPU.

**Metrics.** We use Attack Success Rate (ASR) to evaluate the effectiveness of adversarial examples on VideoQA tasks. It measures the percentage of successful attacks on questions the model answered correctly for clean videos. Answer correctness is evaluated using GPT-4o-mini [32],

Attack	Surrogate Model	Chat-UniVi			LLaVA-NeXT-Video			VideoChat			Video-LLaMA			AASR
		ASR $\uparrow$	Acc. $\downarrow$	Score $\downarrow$	ASR $\uparrow$	Acc. $\downarrow$	Score $\downarrow$	ASR $\uparrow$	Acc. $\downarrow$	Score $\downarrow$	ASR $\uparrow$	Acc. $\downarrow$	Score $\downarrow$	
<b>Clean</b>	/	/	60.89	3.34	/	48.95	2.90	/	60.24	3.42	/	53.81	3.09	/
<b>FMM</b>	Chat-UniVi	16.00*	57.41*	3.18*	16.33	50.38	2.93	13.21	60.75	3.39	21.47	53.31	3.06	16.76
	LLaVA-NeXT-Video	9.22	60.65	3.34	20.48*	47.84*	2.83*	13.49	60.30	3.38	21.32	53.43	3.05	16.13
	VideoChat	8.12	61.81	3.38	15.38	51.30	2.98	14.62*	59.91*	3.35*	20.74	54.08	3.09	14.72
	Video-LLaMA	8.70	61.53	3.36	18.76	49.40	2.89	13.84	60.20	3.38	27.93*	48.39*	2.84*	17.31
<b>Vanilla</b>	Chat-UniVi	<b>52.48*</b>	<b>33.16*</b>	<b>1.98*</b>	19.65	48.04	2.83	13.71	60.11	3.36	22.65	52.16	3.02	27.12
	LLaVA-NeXT-Video	9.63	60.50	3.32	36.85*	38.05*	2.41*	13.71	59.97	3.37	26.51	48.93	2.88	21.67
	VideoChat	8.22	61.50	3.38	15.86	51.11	2.98	35.03*	45.00*	2.69*	19.81	54.67	3.11	19.73
	Video-LLaMA	11.93	58.88	3.26	31.82	41.01	2.52	14.40	59.33	3.34	63.96*	23.88*	1.72*	30.53
<b>I2V</b>	CLIP-L/14	25.17	51.53	2.92	27.39	43.63	2.60	27.13	49.57	2.91	30.51	46.49	2.71	27.55
<b>I2V-MLLM</b>	BLIP-2	<u>43.39</u>	<u>38.72</u>	<u>2.33</u>	<u>40.54</u>	<u>33.84</u>	<u>2.21</u>	<b>63.09</b>	<b>26.08</b>	<b>1.82</b>	<b>74.91</b>	<b>17.07</b>	<b>1.39</b>	<b>55.48</b>
	InstructBLIP	36.74	43.29	2.56	37.61	36.17	2.30	54.26	31.99	2.10	<u>69.90</u>	<u>20.58</u>	<u>1.58</u>	49.63
	MiniGPT-4	38.58	42.10	2.50	<b>41.50</b>	<b>32.98</b>	<b>2.16</b>	<u>56.51</u>	<u>30.49</u>	<u>2.06</u>	68.92	21.37	1.60	<u>51.38</u>

Table 2. The results on the **MSVD-QA** for VideoQA tasks. ASR (%) indicates attack success rate. Acc.(%) denotes the accuracy of the model’s predictions, while the Score represents GPT Score, which assesses the model and assigns a relative score to the predictions on a scale of 1 to 5. AASR represents the average ASR across all target models for each surrogate model. \* indicates white-box attacks. A higher ASR or AASR indicates better adversarial transferability. The highest attack performance for each target model is shown in **bold**, and the second-highest in underline.

Attack	Surrogate Model	Chat-UniVi			LLaVA-NeXT-Video			VideoChat			Video-LLaMA			AASR
		ASR $\uparrow$	Acc. $\downarrow$	Score $\downarrow$	ASR $\uparrow$	Acc. $\downarrow$	Score $\downarrow$	ASR $\uparrow$	Acc. $\downarrow$	Score $\downarrow$	ASR $\uparrow$	Acc. $\downarrow$	Score $\downarrow$	
<b>Clean</b>	/	/	39.62	2.51	/	29.17	2.06	/	38.92	2.50	/	31.42	2.17	/
<b>FMM</b>	Chat-UniVi	23.39*	36.85*	2.36*	24.79	31.60	2.17	9.04	39.44	2.53	32.50	32.03	2.20	22.43
	LLaVA-NeXT-Video	13.20	40.01	2.52	28.62*	29.90*	2.09*	8.52	39.24	2.51	32.27	31.94	2.19	20.65
	VideoChat	12.83	40.52	2.54	25.29	31.10	2.15	15.15*	37.99*	2.46*	30.48	32.56	2.21	20.94
	Video-LLaMA	12.72	40.80	2.55	27.92	30.25	2.12	8.16	39.71	2.53	37.38*	29.60*	2.07*	21.55
<b>Vanilla</b>	Chat-UniVi	<b>55.10*</b>	<b>23.10*</b>	<b>1.68*</b>	27.36	30.09	2.10	9.94	39.52	2.52	32.14	32.24	2.21	31.14
	LLaVA-NeXT-Video	13.36	41.08	2.56	41.90*	24.25*	1.83*	8.50	39.56	2.53	35.23	30.41	2.13	24.75
	VideoChat	11.88	41.35	2.57	25.40	30.72	2.14	27.47*	34.42*	2.29*	31.78	32.58	2.21	24.13
	Video-LLaMA	13.71	40.78	2.55	37.88	26.14	1.91	8.73	39.53	2.52	63.66*	18.07*	1.53*	31.00
<b>I2V</b>	CLIP-L/14	30.05	34.53	2.28	35.62	26.96	1.96	18.83	38.59	2.50	36.16	30.16	2.12	30.17
<b>I2V-MLLM</b>	BLIP-2	<u>41.93</u>	<u>28.42</u>	<u>2.00</u>	<b>49.78</b>	<b>19.34</b>	<b>1.58</b>	<b>62.38</b>	<b>18.72</b>	<b>1.57</b>	<b>78.95</b>	<b>10.68</b>	<b>1.17</b>	<b>58.26</b>
	InstructBLIP	37.37	31.88	2.14	47.96	21.72	1.70	54.78	22.66	1.76	73.04	13.52	1.34	53.29
	MiniGPT-4	38.60	30.94	2.11	<u>49.47</u>	<u>21.12</u>	<u>1.67</u>	<u>56.41</u>	<u>21.95</u>	<u>1.73</u>	<u>73.28</u>	<u>13.63</u>	<u>1.32</u>	<u>54.44</u>

Table 3. The results on the **MSRVTT-QA** for VideoQA tasks. The corresponding metrics and settings are consistent with those in Tab. 2.

which checks whether the model’s prediction semantically aligns with the ground truth. We also provide the average ASR (AASR) across all evaluated V-MLLMs. A higher ASR or AASR indicates better adversarial transferability. To evaluate the model’s overall performance when encountering adversarial videos, we further employ GPT-assisted methods [29] to assess Accuracy (Acc.) and GPT-Score. Specifically, accuracy (Acc.) refers to the model’s prediction accuracy, while the GPT score (Score) assesses the quality of the model’s predictions, assigning a relative score on a scale from 1 to 5. GPT-4o-mini is used for evaluation due to its strong text understanding and cost efficiency. For detailed explanations of the metrics, see the Appendix B.

## 4.2. Attack performance

In this section, we compare our proposed I2V-MLLM attack with the FMM, Vanilla, and I2V attacks. The results, sum-

marized in Tab. 2 and Tab. 3, provide a quantitative comparison of the ASR, AASR, Acc., and GPT Score for the MSVD-QA and MSRVTT-QA datasets, respectively.

**Evaluation of ASR.** As shown in Tab. 2 and Tab. 3, I2V-MLLM achieves the best and near-best attack performance on the LLaVa-NeXT-Video, VideoChat, and Video-LLaMA. It attains ASR of 41.50%, 63.09%, and 74.91% for MSVD-QA, 49.78%, 62.38%, and 78.95% for MSRVTT-QA, respectively, even surpassing Vanilla and FMM attack methods in the white-box setting. For Chat-UniVi, I2V-MLLM achieves a suboptimal ASR of 43.39% for MSVD-QA and 41.93% for MSRVTT-QA, slightly below the Vanilla attack’s ASR of 52.48% for MSVD-QA and 55.10% for MSRVTT-QA in the white-box setting. These results demonstrate that I2V-MLLM performs better in the black-box setting, with its generated adversarial videos showing stronger cross-model transferability.

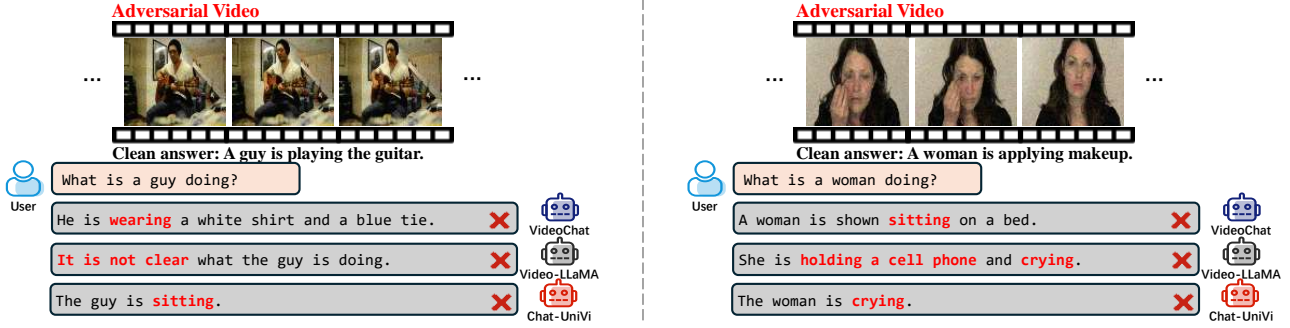


Figure 3. The adversarial video samples for VideoQA tasks are based on MSVD-QA, where the surrogate model is BLIP-2 and the target V-MLLMs are VideoChat, Video-LLaMA, and Chat-UniVi. The clean answers are the responses generated by Chat-UniVi on clean video samples. Red crosses indicate that the responses generated by V-MLLMs do not semantically align with the expected clean answers.

Type	Correct	Detail	Context	Temporal	Consistency
Clean	2.38	2.54	2.97	1.97	1.88
Vanilla	2.16	2.29	2.71	1.62	1.86
Vanilla*	<b>2.07</b>	<u>2.25</u>	<b>2.64</b>	<b>1.55</b>	<b>1.74</b>
I2V-MLLM	<u>2.10</u>	<b>2.23</b>	<u>2.69</u>	<b>1.55</b>	<u>1.83</u>

Table 4. The results on the **ActivityNet-200** for video understanding tasks. All scores range from 1 to 5, with lower scores indicating better attack performance. \* indicates a white-box attack. The highest attack performance is shown in **bold**, and the second-highest in underline.

V- MLLM	$\lambda_1 : \lambda_2$				
	1:1	1:2	1:3	2:1	3:1
Chat-UniVi	<b>43.11</b>	43.09	41.91	42.14	41.35
LLaVA-NeXT-Video	35.67	34.08	33.12	35.25	<b>35.96</b>
VideoChat	<b>51.10</b>	49.50	49.03	49.72	50.44
Video-LLaMA	<b>64.57</b>	64.11	62.98	63.56	61.94
AASR	<b>48.61</b>	47.69	46.76	47.67	47.42

Table 5. ASR (%) of the I2V-MLLM attack across different weight ratios of the vision model loss ( $\lambda_1$ ) and projector loss ( $\lambda_2$ ). A higher AASR indicates better adversarial transferability.

Alternatively, I2V-MLLM achieves the highest AASR compared to previous attack methods, achieving AASR of 55.48%, 49.63%, and 51.38% for MSVD-QA and 58.26%, 53.29%, and 54.44% for MSRVTT-QA when taking BLIP-2, InstructBLIP, MiniGPT-4 as surrogate models, respectively, significantly outperforming previous attack methods. This highlights that I2V-MLLM is capable of steadily generating high-quality adversarial video samples that deceive the unseen V-MLLMs.

**Evaluation of the quality of generated answers.** We also incorporate Acc. and GPT Score as metrics to better analyze the impact of adversarial videos on V-MLLM performance. As shown in Tab. 2 and Tab. 3, the proposed I2V-MLLM significantly reduces both Acc. and Scores across

all target models, particularly for VideoChat and Video-LLaMA. On the MSVD-QA dataset, Acc. drops to 26.08% and 17.07%, while Scores fall to 1.82 and 1.39. On the MSRVTT-QA dataset, Acc. further declines to 18.72% and 10.68%, with Scores of 1.57 and 1.17, respectively. Significant effects are also observed on Chat-UniVi and LLaVA-NeXT-Video. These significant performance degradations highlight the destructive power of the I2V-MLLM attack, demonstrating its transferability and effectiveness across multiple V-MLLMs, while revealing the adversarial vulnerability of existing models, even in black-box settings.

As shown in Fig. 3, adversarial video samples generated from the I2V-MLLM attack cause V-MLLMs to produce responses that differ significantly from the clean answers, demonstrating that our method effectively misleads V-MLLMs and disrupts their ability to accurately interpret the video content.

### 4.3. Results on video understanding tasks

Video understanding tasks assess whether V-MLLMs have comprehended the content of a video by posing a range of questions about it. Following Maaz et al. [29], we use a subset of the ActivityNet-200 [15] dataset and employ GPT-4o-mini to evaluate the model’s responses to adversarial examples from five perspectives: Correctness, Detail Orientation, Contextual Understanding, Temporal Understanding, and Consistency. We compare our proposed I2V-MLLM attack with the Vanilla attack on LLaVA-NeXT-Video, using clean samples as a reference. Evaluations are performed on three attack types: white-box Vanilla attack, black-box Vanilla attack (using Video-LLaMA as a surrogate model), and I2V-MLLM attack (using BLIP-2 as a surrogate model).

As shown in Tab. 4, the black-box Vanilla attack induces minimal disruption, while the white-box Vanilla attack leads to the most significant interference. The I2V-MLLM performs similarly to the white-box Vanilla attack in terms of Correct, Detail, Context, and Temporal aspects,

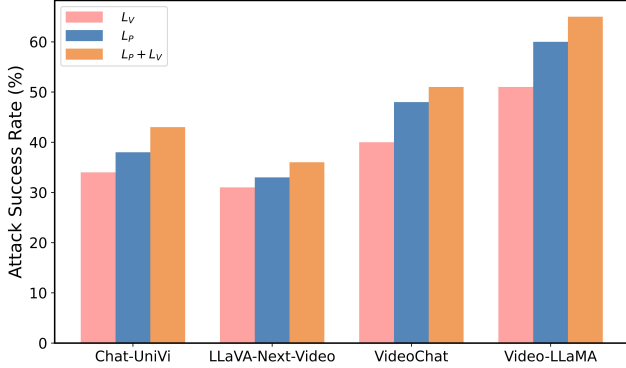


Figure 4. ASR (%) of the I2V-MLLM attack with different loss functions.

with only a drawback in Consistency. These results show that I2V-MLLM achieves comparable performance to the white-box Vanilla attack on video understanding tasks, further validating its effectiveness and transferability.

#### 4.4. Ablation study

In this section, we provide ablation studies on the objective function, step size  $\alpha$ , number of iterations  $I$ , key-frame ratio  $\beta$ , and perturbation propagation in I2V-MLLM attack. Experiments are conducted on the MSVD-QA dataset for VideoQA tasks. We use BLIP-2 as the surrogate model and four different V-MLLMs as black-box models.

**Influence of loss functions and weight ratio.** In Fig. 4, we provide ablation study on the components of the objective function used in our I2V-MLLM. The surrogate model is BLIP-2, and the generated adversarial videos are evaluated across four V-MLLMs. It can be observed that using either  $\mathcal{L}_V$  or  $\mathcal{L}_P$  alone achieves satisfactory attack performance. Combining both, which simultaneously disrupts low-level image features and the alignment between visual and textual modalities, further enhances the attack performance. We also vary the weights of the  $\mathcal{L}_V$  and  $\mathcal{L}_P$  to explore their relative relationship. As shown in Tab. 5, the AASR is highest when the ratio of  $\lambda_1$  to  $\lambda_2$  is 1:1. Therefore, we adopt this weight ratio in our experiments.

**Influence of step size and iteration number.** We utilize the PGD to update the perturbations, which is influenced by the step size  $\alpha$  and the number of iterations  $I$ . Fig. 5 presents the results obtained with a key-frame ratio  $\beta = 10\%$  under different step sizes and iteration numbers. It can be observed that as the number of iterations  $I$  increases, the transferability (ASR) of adversarial examples improves, and when the iterations exceed 50, the benefits from further increases gradually diminish. A similar pattern is observed with the step size selection. Moderate values of  $\alpha$  and  $I$  yield best AASR. To achieve optimal performance, we adopt  $\alpha = 1$  and  $I = 50$  in our experiments.

**Influence of key-frame ratio and propagation.** The

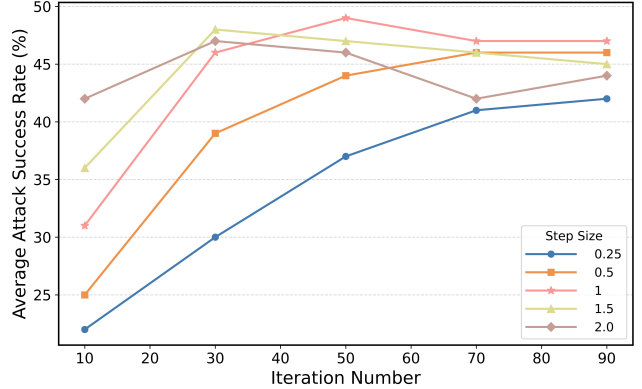


Figure 5. AASR (%) of the I2V-MLLM attack with various step sizes and iteration numbers.

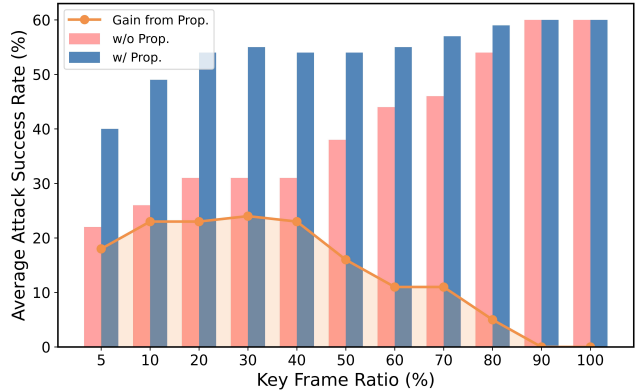


Figure 6. AASR (%) of the I2V-MLLM attack with various key-frame ratios, comparing scenarios with and without perturbation propagation. ‘Prop.’ represents ‘Propagation’.

number of key-frames used to optimize the perturbation, as well as the decision to propagate these perturbations across the entire video, significantly affects the transferability of adversarial video samples. Fig. 6 illustrates the results obtained with various key-frame ratios, comparing scenarios with and without perturbation propagation. It can be observed that as the key frame ratio increases, the generated adversarial samples show improved transferability. On the other hand, perturbation propagation substantially improves AASR by ensuring that all the frames extracted by unseen V-MLLMs are perturbed. As illustrated by the gain curve in the Fig. 6, the improvement from perturbation propagation initially rises with the key-frame ratio but then diminishes, reaching its maximum at 30%. With an AASR already high at a 30% key-frame ratio, further increases yield minimal gains, and perturbation propagation reaches its maximal benefit at this point. Therefore, we adopt a key-frame ratio of  $\beta = 30\%$ . More experiments and analysis can be found in the Appendix B.



## 5. Conclusion

In this paper, we are the first to explore black-box transferable attacks on V-MLLMs. We conduct a thorough investigation of the limitations of existing methods, revealing that they exhibit lower transferability despite their impressive performance in white-box settings. Our findings underscore the need for specially designed transferable attacks tailored to V-MLLMs. We propose the I2V-MLLM attack, a highly transferable cross-modal attack that leverages the intermediate features of IMMs and perturbation propagation to enhance the transferability of attacks targeting V-MLLMs. We hope our work will inspire further research aimed at evaluating and improving the robustness of V-MLLMs.

## References

- [1] Jean-Baptiste Alayrac, Jeff Donahue, Pauline Luc, Antoine Miech, Iain Barr, Yana Hasson, Karel Lenc, Arthur Mensch, Katie Millican, Malcolm Reynolds, Roman Ring, Eliza Rutherford, Serkan Cabi, Tengda Han, Zhitao Gong, Sina Samangooei, Marianne Monteiro, Jacob Menick, Sebastian Borgeaud, Andrew Brock, Aida Nematzadeh, Sahand Sharifzadeh, Mikolaj Binkowski, Ricardo Barreira, Oriol Vinyals, Andrew Zisserman, and Karen Simonyan. Flamingo: a visual language model for few-shot learning, 2022. 2
- [2] Anas Awadalla, Irena Gao, Josh Gardner, Jack Hessel, Yusuf Hanafy, Wanrong Zhu, Kalyani Marathe, Yonatan Bitton, Samir Gadre, Shiori Sagawa, Jenia Jitsev, Simon Kornblith, Pang Wei Koh, Gabriel Ilharco, Mitchell Wortsman, and Ludwig Schmidt. Openflamingo: An open-source framework for training large autoregressive vision-language models, 2023.
- [3] Jinze Bai, Shuai Bai, Shusheng Yang, Shijie Wang, Sinan Tan, Peng Wang, Junyang Lin, Chang Zhou, and Jingren Zhou. Qwen-vl: A versatile vision-language model for understanding, localization, text reading, and beyond, 2023. 2
- [4] Luke Bailey, Euan Ong, Stuart Russell, and Scott Emmons. Image hijacks: Adversarial images can control generative models at runtime. *arXiv preprint arXiv:2309.00236*, 2023. 2
- [5] Yuxin Cao, Xi Xiao, Ruoxi Sun, Derui Wang, Minhui Xue, and Sheng Wen. Stylefool: Fooling video classification systems via style transfer. In *2023 IEEE symposium on security and privacy (SP)*, pages 1631–1648. IEEE, 2023. 3
- [6] Yuxin Cao, Ziyu Zhao, Xi Xiao, Derui Wang, Minhui Xue, and Jin Lu. Logostylefool: Vitiating video recognition systems via logo style transfer, 2024. 3
- [7] Wei-Lin Chiang, Zhuohan Li, Zi Lin, Ying Sheng, Zhanghao Wu, Hao Zhang, Lianmin Zheng, Siyuan Zhuang, Yonghao Zhuang, Joseph E. Gonzalez, Ion Stoica, and Eric P. Xing. Vicuna: An open-source chatbot impressing gpt-4 with 90%\* chatgpt quality, 2023. 5, 1
- [8] Xuanming Cui, Alejandro Aparcedo, Young Kyun Jang, and Ser-Nam Lim. On the robustness of large multimodal models against image adversarial attacks, 2023. 2
- [9] Wenliang Dai, Junnan Li, Dongxu Li, Anthony Meng Huat Tiong, Junqi Zhao, Weisheng Wang, Boyang Li, Pascale Fung, and Steven Hoi. Instructblip: Towards general-purpose vision-language models with instruction tuning, 2023. 1, 2, 5
- [10] Yinpeng Dong, Fangzhou Liao, Tianyu Pang, Hang Su, Jun Zhu, Xiaolin Hu, and Jianguo Li. Boosting adversarial attacks with momentum. In *2018 IEEE/CVF Conference on Computer Vision and Pattern Recognition*, 2018. 2, 3
- [11] Yinpeng Dong, Huanran Chen, Jiawei Chen, Zhengwei Fang, Xiao Yang, Yichi Zhang, Yu Tian, Hang Su, and Jun Zhu. How robust is google’s bard to adversarial image attacks?, 2023. 2
- [12] Mingjing Du, Shifei Ding, and Hongjie Jia. Study on density peaks clustering based on k-nearest neighbors and principal component analysis. *Knowledge-Based Systems*, page 135–145, 2016. 2
- [13] Xiaohan Fu, Zihan Wang, Shuheng Li, Rajesh K. Gupta, Niloofar Mireshghallah, Taylor Berg-Kirkpatrick, and Earlene Fernandes. Misusing tools in large language models with visual adversarial examples, 2023. 2
- [14] Google. Gemini, 2024. 2
- [15] Fabian Caba Heilbron, Victor Escorcia, Bernard Ghanem, and Juan Carlos Niebles. Activitynet: A large-scale video benchmark for human activity understanding. In *2015 IEEE Conference on Computer Vision and Pattern Recognition (CVPR)*, 2015. 2, 5, 7, 4
- [16] Wenbo Hu, Yifan Xu, Yi Li, Weiye Li, Zeyuan Chen, and Zhuowen Tu. Bliva: A simple multimodal llm for better handling of text-rich visual questions, 2023. 2
- [17] Linxi Jiang, Xingjun Ma, Shaoxiang Chen, James Bailey, and Yu-Gang Jiang. Black-box adversarial attacks on video recognition models. In *Proceedings of the 27th ACM International Conference on Multimedia*, pages 864–872, 2019. 3
- [18] Peng Jin, Ryuichi Takanobu, Wancai Zhang, Xiaochun Cao, and Li Yuan. Chat-univi: Unified visual representation empowers large language models with image and video understanding, 2024. 1, 2, 3, 5
- [19] Hee-Seon Kim, Minji Son, Minbeom Kim, Myung-Joon Kwon, and Changick Kim. Breaking temporal consistency: Generating video universal adversarial perturbations using image models, 2023. 2, 3
- [20] Junnan Li, Dongxu Li, Silvio Savarese, and Steven Hoi. Blip-2: Bootstrapping language-image pre-training with frozen image encoders and large language models, 2023. 3, 5, 1
- [21] Jinmin Li, Kuofeng Gao, Yang Bai, Jingyun Zhang, Shu tao Xia, and Yisen Wang. Fmm-attack: A flow-based multimodal adversarial attack on video-based llms, 2024. 1, 2, 3, 4
- [22] KunChang Li, Yanan He, Yi Wang, Yizhuo Li, Wenhai Wang, Ping Luo, Yali Wang, Limin Wang, and Yu Qiao. Videochat: Chat-centric video understanding, 2024. 1, 2, 5
- [23] Shasha Li, Ajaya Neupane, Sujoy Paul, Chengyu Song, Srikanth V Krishnamurthy, Amit K Roy Chowdhury, and

- Ananthram Swami. Adversarial perturbations against real-time video classification systems. *arXiv preprint arXiv:1807.00458*, 2018. 3
- [24] Bin Lin, Yang Ye, Bin Zhu, Jiayi Cui, Munan Ning, Peng Jin, and Li Yuan. Video-llava: Learning united visual representation by alignment before projection, 2024. 1
- [25] Jiadong Lin, Chuanbiao Song, Kun He, Liwei Wang, and John E. Hopcroft. Nesterov accelerated gradient and scale invariance for adversarial attacks, 2020. 2, 3
- [26] Haotian Liu, Chunyuan Li, Qingyang Wu, and Yong Jae Lee. Visual instruction tuning, 2023. 2
- [27] Dong Lu, Zhiqiang Wang, Teng Wang, Weili Guan, Hongchang Gao, and Feng Zheng. Set-level guidance attack: Boosting adversarial transferability of vision-language pre-training models. In *Proceedings of the IEEE/CVF International Conference on Computer Vision*, pages 102–111, 2023. 2
- [28] Haochen Luo, Jindong Gu, Fengyuan Liu, and Philip Torr. An image is worth 1000 lies: Adversarial transferability across prompts on vision-language models, 2024. 2
- [29] Muhammad Maaz, Hanoona Rasheed, Salman Khan, and Fahad Shahbaz Khan. Video-chatgpt: Towards detailed video understanding via large vision and language models, 2024. 1, 2, 4, 5, 6, 7
- [30] Aleksander Madry, Aleksandar Makelov, Ludwig Schmidt, Dimitris Tsipras, and Adrian Vladu. Towards deep learning models resistant to adversarial attacks, 2019. 5
- [31] Microsoft. Bing Chat, 2024. 2
- [32] OpenAI. GPT-4o-Mini: Advancing Cost-Efficient Intelligence, 2024. 3, 5, 2
- [33] OpenAI. GPT-4V(ision) System Card, 2024. 2
- [34] Alec Radford, Jong Wook Kim, Chris Hallacy, Aditya Ramesh, Gabriel Goh, Sandhini Agarwal, Girish Sastry, Amanda Askell, Pamela Mishkin, Jack Clark, Gretchen Krueger, and Ilya Sutskever. Learning transferable visual models from natural language supervision, 2021. 5
- [35] Josef Schmee. An introduction to multivariate statistical analysis. *Technometrics*, page 180–181, 1986. 5
- [36] Haoqin Tu, Chenhang Cui, Zijun Wang, Yiyang Zhou, Bingchen Zhao, Junlin Han, Wangchunshu Zhou, Huaxiu Yao, and Cihang Xie. How many unicorns are in this image? a safety evaluation benchmark for vision llms. *arXiv preprint arXiv:2311.16101*, 2023. 2
- [37] Ruikui Wang, Yuanfang Guo, and Yunhong Wang. Global-local characteristic excited cross-modal attacks from images to videos. In *Proceedings of the AAAI Conference on Artificial Intelligence*, pages 2635–2643, 2023. 2, 3
- [38] Zhipeng Wei, Jingjing Chen, Xingxing Wei, Linxi Jiang, Tat-Seng Chua, Fengfeng Zhou, and Yu-Gang Jiang. Heuristic black-box adversarial attacks on video recognition models. In *Proceedings of the AAAI Conference on Artificial Intelligence*, pages 12338–12345, 2020. 3
- [39] Zhipeng Wei, Jingjing Chen, Zuxuan Wu, and Yu-Gang Jiang. Cross-modal transferable adversarial attacks from images to videos, 2021. 2, 3, 4, 1
- [40] Shangyu Xie, Han Wang, Yu Kong, and Yuan Hong. Universal 3-dimensional perturbations for black-box attacks on video recognition systems. In *2022 IEEE Symposium on Security and Privacy (SP)*, pages 1390–1407. IEEE, 2022. 3
- [41] Dejing Xu, Zhou Zhao, Jun Xiao, Fei Wu, Hanwang Zhang, Xiangnan He, and Yueting Zhuang. Video question answering via gradually refined attention over appearance and motion. In *ACM Multimedia*, 2017. 2, 5
- [42] Hang Zhang, Xin Li, and Lidong Bing. Video-llama: An instruction-tuned audio-visual language model for video understanding, 2023. 1, 2, 3, 5
- [43] Hao Zhang, Wenqi Shao, Hong Liu, Yongqiang Ma, Ping Luo, Yu Qiao, and Kaipeng Zhang. Avibench: Towards evaluating the robustness of large vision-language model on adversarial visual-instructions. *arXiv preprint arXiv:2403.09346*, 2024. 2
- [44] Yuanhan Zhang, Jinming Wu, Wei Li, Bo Li, Zejun Ma, Ziwei Liu, and Chunyuan Li. Video instruction tuning with synthetic data, 2024. 2, 5, 1
- [45] Yunqing Zhao, Tianyu Pang, Chao Du, Xiao Yang, Chongxuan Li, Ngai-Man Cheung, and Min Lin. On evaluating adversarial robustness of large vision-language models, 2023. 2
- [46] Deyao Zhu, Jun Chen, Xiaoqian Shen, Xiang Li, and Mohamed Elhoseiny. Minigt-4: Enhancing vision-language understanding with advanced large language models, 2023. 2, 3, 5, 1

# Image-based Multimodal Models as Intruders: Transferable Multimodal Attacks on Video-based MLLMs

## Supplementary Material

### A. Motivation

To improve the transferability of attacks on V-MLLMs, we first conduct a thorough investigation into the shortcomings of existing methods, as showed in Tab.1 of the main content. Based on the experimental results, we summarize the shortcomings of these existing methods as follows: (1) focusing only on sparse key-frames, (2) lacking generalization in perturbing video features, and (3) failing to integrate multimodal information.

**Focusing only on sparse key-frames.** The FMM attack [21] is the first white-box attack targeting V-MLLMs, using a flow-based temporal mask to perturb selected key frames and disrupt video and LLM features. As shown in Tab.1 of the main content, however, its adversarial transferability is limited due to differences in key-frame selection between the attack and V-MLLMs. Since V-MLLMs may sample unperturbed frames, we replaced the flow-based mask with direct perturbations on key frames sampled by V-MLLMs, calling this the *vanilla* attack. The comparison between the FMM and vanilla attacks in Tab.1 of the main content shows a marked improvement in white-box performance after the adjustment. However, the transferability remains limited due to diverse frame-sampling strategies in V-MLLMs. Extending key-frame perturbations to the entire video further improves transferability, as shown in rows 1, 2, 4, and 5 of Tab.1 of the main content. These results emphasize the need to perturb all frames sampled by V-MLLMs for optimal attack performance.

**Lacking generalization in perturbing video features.** The gains from perturbation propagation are limited due to variations in how V-MLLMs extract video features, which often causes the perturbations to overfit to the features of the surrogate model’s video encoder, which reduces the generalizability of perturbations. Enhancing transferability requires targeting common elements across these features. Thus, we focus on lower-level image features. The I2V attack [39], which perturbs each video frame to disrupt image features, demonstrates that using image models as surrogates can effectively generate adversarial samples for video models. Experimental results in row 3, 4 and 5 of Tab.1 of the main content confirm that targeting image features in video frames significantly improves the transferability of adversarial samples.

**Failing to integrate multimodal information.** The I2V attack was initially developed for video classification tasks and does not consider the multimodal interactions between video and text, which are crucial for comprehensive video

understanding. While I2V attack achieves improved transferability, its effectiveness in video understanding tasks remains limited. Therefore, we propose using an image-based multimodal model as a surrogate, integrating multimodal interaction information into the process of generating adversarial video samples, which leads to a significant improvement in transferability, as demonstrated in the rows 3 and 6 of Tab.1 of the main content.

In summary, we propose using IMM as surrogates to generate adversarial video samples that incorporate multimodal interactions. In addition, we introduce a perturbation propagation technique to handle different unknown frame sampling strategies. The I2V-MLLM results in Tab.1 of the main content demonstrate the strong transferability of our method across different V-MLLMs.

### B. Experiment & Analysis

#### B.1. Experiment setting

In this section, we provide a more detailed description of the experiment setting.

**Surrogate models.** We perform our proposed approach on three IMM: BLIP-2 [20], InstructBLIP [9] and MiniGPT-4 [46]. BLIP-2 employs a novel pre-training strategy that integrates frozen pre-trained image encoders and language models, effectively bridging the modality gap with a lightweight Q-Former. InstructBLIP enhances BLIP-2 by introducing vision-language instruction tuning. It uses a diverse range of datasets and an instruction-aware Q-Former to extract relevant features, improving task performance. MiniGPT-4 aligns a frozen visual encoder with the LLMs, achieving a seamless integration that enhances its multimodal capabilities and demonstrates the potential of such alignments in advancing multimodal understanding.

**Target models.** Our proposed methods are evaluated on four different V-MLLMs: Chat-UniVi [18], LLaVA-Next-Video [44], VideoChat [22] and Video-LLaMA [42], each with a Vicuna-7B [7] as the LLM. Chat-UniVi uses dynamic visual tokens for uniform representation of images and videos, efficiently capturing spatial details and temporal relationships through a multi-scale framework. LLaVA-Next-Video is an open-source chatbot that enhances large language models by fine-tuning them on multimodal instruction-following data. VideoChat combines video foundation models and LLMs with a learnable neural interface, excelling in spatiotemporal reasoning and event localization. Video-LLaMA uses a multi-modal framework that

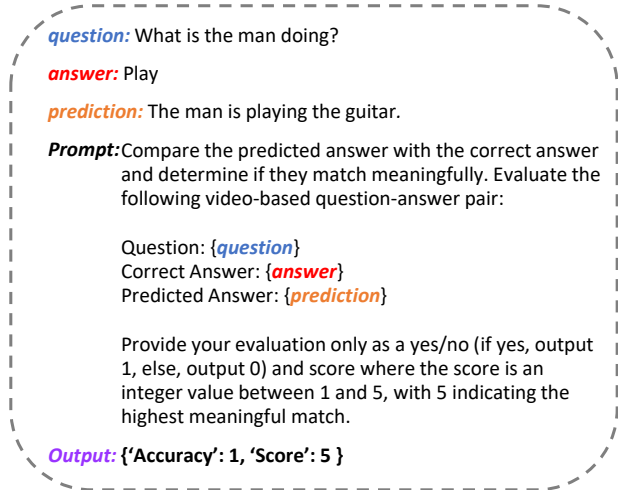


Figure 7. An example of using GPT-4o-mini to evaluate Accuracy and GPT Score for the VideoQA task, following the methodology in [29].

improves LLMs’ understanding of visual and auditory content in videos, employing a Video Q-former to create video encoders and introducing a video-to-text generation task to learn video-language correspondence.

**Metrics.** We use Attack Success Rate (ASR) to evaluate the effectiveness of adversarial examples on VideoQA tasks. It measures the percentage of successful attacks on questions the model answered correctly for clean videos. Answer correctness is evaluated using GPT-4o-mini [32], which checks whether the model’s prediction semantically aligns with the ground truth. We also provide the average ASR (AASR) across all evaluated V-MLLMs. A higher ASR or AASR indicates better adversarial transferability. To evaluate the model’s overall performance when encountering adversarial videos, we further employ GPT-assisted methods [29] to assess Accuracy (Acc.) and GPT-Score. We use GPT-4o-mini [32] as the evaluation model due to its superior performance in text understanding and its cost efficiency.

Fig. 7 illustrates an example of evaluating the VideoQA task with GPT-4o-mini. An adversarial attack is considered successful if the adversarial video sample causes the V-MLLM to change its response to a question from correct (Accuracy: 1) to incorrect (Accuracy: 0).

## B.2. Boosting adversarial transferability

To boost adversarial transferability on VideoQA tasks, we draw inspiration from image classification and explore transfer-based attack techniques. Specifically, we consider the Momentum Iterative (MI) method [10], which incorporates momentum to stabilize and diversify gradient updates, and the Nesterov Iterative (NI) method [25], which lever-

ages Nesterov acceleration to refine gradient smoothing and explore a broader adversarial space.

As shown in Tab. 6, the addition of MI and NI does not significantly improve the transferability of FMM and Vanilla methods; instead, it slightly reduces their performance. In particular, NI greatly decreases the attack effectiveness in white-box scenarios, as it smooths the gradients to improve generalization, which inadvertently compromises precision in white-box scenarios.

Although MI and NI do not enhance the attack performance of methods using V-MLLMs as surrogate models, they improve the performance of I2V and I2V-MLLM methods that leverage image models as surrogates. Specifically, NI increases the ASR of I2V against Chat-UniVi from 30.05% to 39.89%, improves the AASR of I2V from 30% to 34.67%, boosts the ASR of I2V-MLLM against Video-LLaMA from 74.91% to 83.08%, and raises the AASR of I2V-MLLM from 55.48% to 60.67%. With the incorporation of MI and NI, the proposed I2V-MLLM method still achieves a significantly higher AASR compared to other methods, further demonstrating its strong transferability and effectiveness in attacking various V-MLLMs.

## B.3. Ablation study

The experiments in this section are conducted on the MSVD-QA validation set, using BLIP-2 as the surrogate model. A higher ASR or AASR reflects better adversarial transferability.

**Influence of input text.** When designing  $\mathcal{L}_{P_{v2t}}$  in Eq. (4) of the main content, we consider two types of text inputs: questions and captions generated from the questions and their answers. As illustrated in Fig. 8, we use GPT-4o-mini to generate caption based on the question and answer. The experiment results are shown in Tab. 7, using captions as input yields a slightly higher AASR compared to using questions. This is because captions contain answer-related information, and the perturbations introduced during the iterations disrupt the semantic information within the answers, making it more challenging for V-MLLMs to provide responses aligned with the ground truth.

**Influence of vision model loss function.** In Sec.3.3.1, Eq. (2) defines the loss function for the vision model attack, which can be further decomposed into  $\mathcal{L}_V = \mathcal{L}_V^s + \mathcal{L}_V^t$ .

To disrupt video-level spatial features, I2V-MLLM generates adversarial perturbations by minimizing the cosine similarity between the original and adversarial spatial features:

$$\mathcal{L}_V^s = \sum_{i=1}^K \frac{\text{Cos}(F_V^s(X)_i, F_V^s(X_{adv})_i)}{K}, \quad (8)$$

where  $F_V^s(X)_i$  and  $F_V^s(X_{adv})_i$  denote the  $i$ -th elements of the spatial features extracted from the original and adversarial video frames, respectively.

Attack	Surrogate Model	Chat-UniVi	LLaVA-NeXT-Video	VideoChat	Video-LLaMA	AASR
<b>FMM</b>	Chat-UniVi	16.00*	16.34	13.21	21.47	16.76
	LLaVA-NeXT-Video	9.22	20.48*	13.49	21.32	16.13
	VideoChat	8.12	15.38	14.62*	20.74	14.72
	Video-LLaMA	8.70	18.76	13.84	27.93*	17.31
<b>FMM + MI</b>	Chat-UniVi	9.63*	17.55	13.12	21.47	15.44
	LLaVA-NeXT-Video	8.76	21.72*	13.37	22.22	16.52
	VideoChat	7.76	15.86	14.97*	20.74	14.83
	Video-LLaMA	8.76	19.75	13.31	28.74*	17.64
<b>FMM + NI</b>	Chat-UniVi	13.39*	17.55	13.24	21.61	16.45
	LLaVA-NeXT-Video	8.88	20.80*	13.62	23.06	16.59
	VideoChat	7.71	15.73	13.37*	19.99	14.2
	Video-LLaMA	8.29	19.39	13.43	22.13*	15.81
<b>Vanilla</b>	Chat-UniVi	<b>52.48*</b>	19.65	13.71	22.65	27.12
	LLaVA-NeXT-Video	9.63	36.85*	13.71	26.51	21.67
	VideoChat	8.22	15.86	35.03*	19.81	19.73
	Video-LLaMA	11.93	31.82	14.40	63.96*	30.53
<b>Vanilla + MI</b>	Chat-UniVi	45.26*	21.05	13.99	22.91	25.05
	LLaVA-NeXT-Video	8.96	45.44*	13.71	27.87	23.50
	VideoChat	7.55	15.99	40.36*	21.12	21.51
	Video-LLaMA	11.78	43.06	13.24	72.22*	35.57
<b>Vanilla + NI</b>	Chat-UniVi	14.34*	19.14	13.46	21.23	17.04
	LLaVA-NeXT-Video	8.45	23.54*	13.31	24.71	17.75
	VideoChat	7.09	15.83	16.88*	19.90	14.94
	Video-LLaMA	8.86	26.72	12.87	28.53*	19.50
<b>I2V</b>		30.05	35.62	18.83	30.16	30.17
<b>I2V + MI</b>	CLIP-L/14	25.88	34.97	19.63	30.39	27.72
<b>I2V + NI</b>		39.89	39.46	24.48	34.85	34.67
<b>I2V-MLLM</b>		43.39	40.54	<u>63.09</u>	<u>74.91</u>	55.48
<b>I2V-MLLM + MI</b>	BLIP-2	<u>48.39</u>	<b>54.71</b>	62.18	73.75	<u>59.76</u>
<b>I2V-MLLM + NI</b>		43.52	<u>49.36</u>	<b>66.72</b>	<b>83.08</b>	<b>60.67</b>

Table 6. ASR(%) of different attacks on the **MSVD-QA** for VideoQA tasks. AASR represents the average ASR across all target models for each surrogate model. \* indicates white-box attacks. A higher ASR or AASR indicates better adversarial transferability. MI [10] refers to the Momentum Iterative method, which enhances gradient diversity by incorporating momentum. NI [25] denotes the Nesterov Iterative method, which improves transferability by smoothing gradients and exploring broader search spaces. The highest attack performance for each target model is shown in **bold**, and the second-highest in underline.

**question:** What is the man doing?  
**answer:** eat  
**Prompt:** Transform the **question** and **answer** into a declarative sentence and only output the declarative sentence.  
**Output:** The man is eating.

Figure 8. An example of utilizing GPT-4o-mini to generate a caption based on the question and its corresponding answer.

Target Model	Caption	Question
Chat-UniVi	<b>0.45</b>	0.44
LLaVA-NeXT-Video	<b>0.36</b>	0.35
VideoChat	<b>0.51</b>	0.50
Video-LLaMA	<b>0.65</b>	0.65
<b>AASR</b>	<b>0.49</b>	0.48

Table 7. This table presents the ASR (%) across different V-MLLMs under varying input text types. The highest attack performance for each target model is shown in **bold**.

Similarly, to disrupt video-level temporal features, I2V-MLLM minimizes the cosine similarity between the original and adversarial temporal features:

$$\mathcal{L}_V^t = \sum_{i=1}^N \frac{\text{Cos}(F_V^t(X)_i, F_V^t(X_{adv})_i)}{N}, \quad (9)$$

where  $F_V^t(X)_i$  and  $F_V^t(X_{adv})_i$  represent the  $i$ -th elements of the temporal features for the original and adversarial video frames, respectively.

We analyze the individual influence of the components of  $\mathcal{L}_V$ . As illustrated in Fig. 9, the combination of  $\mathcal{L}_V^s$  and  $\mathcal{L}_V^t$  results in an improvement in ASR, highlighting the effectiveness of  $\mathcal{L}_V$  in leveraging the spatiotemporal information of video samples to craft adversarial perturbations.

**Influence of projector loss function.** We examine the influence of components of  $\mathcal{L}_P$ . As illustrated in Fig. 10, the combination of  $\mathcal{L}_{P_v}$  and  $\mathcal{L}_{P_{v2t}}$  leads to an improvement in ASR, demonstrating the effectiveness of  $\mathcal{L}_P$  in leveraging the multimodal interactions between video and text to craft adversarial perturbations.

**Influence of weights of loss functions.** We vary the weights of the  $\mathcal{L}_V$  and  $\mathcal{L}_P$  to explore their relative relationship. As shown in Tab. 8, the AASR is highest when the ratio of  $\lambda_1$  to  $\lambda_2$  is 1:1. Therefore, we adopt this weight ratio in our experiments.

**Results on video understanding tasks.** Video understanding tasks assess whether V-MLLMs have comprehended the content of a video by posing a range of questions about it. Following Maaz et al. [29], we use a subset

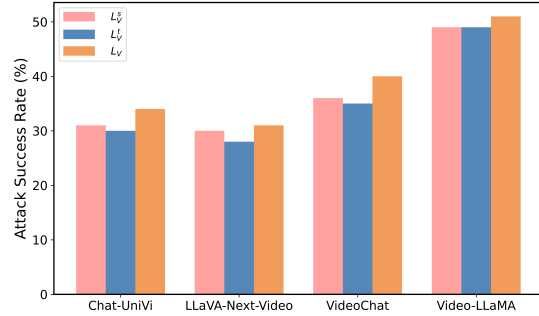


Figure 9. ASR (%) of vision model attacks in I2V-MLLM with different loss functions.

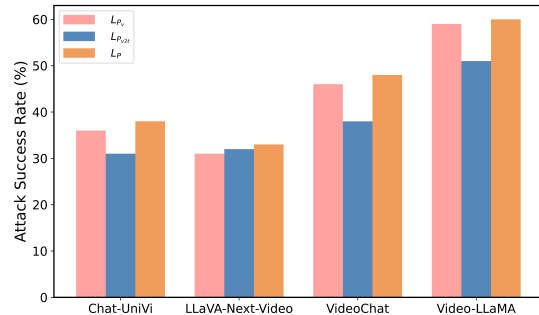


Figure 10. ASR (%) of projector attacks in I2V-MLLM with different loss functions.

of the ActivityNet-200 [15] dataset and employ GPT-4o-mini to evaluate the model’s responses to adversarial examples from five perspectives: Correctness, Detail Orientation, Contextual Understanding, Temporal Understanding, and Consistency. We compare our proposed I2V-MLLM attack with the Vanilla attack on four V-MLLMs, using clean samples as a reference. Evaluations are performed on white-box Vanilla attack and I2V-MLLM attack (using BLIP-2 as a surrogate model).

As shown in Tab. 9, I2V-MLLM achieves performance comparable to the white-box Vanilla attack and even outperforms it on VideoChat and Video-LLaMA, further validating its effectiveness and transferability.

## B.4. Analysis

In this section, we will discuss the consistency of intermediate features between IMM and V-MLLM, as well as present more cases of successful adversarial attacks.

**Discussion.** To experimentally validate the effectiveness of Eq (6) in the main content, we analyze how the cosine similarity between adversarial and benign features in

Target Model	$\lambda_1 : \lambda_2$								
	1:1	1:2	1:3	1:4	1:5	2:1	3:1	4:1	5:1
Chat-UniVi	<b>43.11</b>	43.09	41.91	43.16	40.91	42.14	41.35	40.66	40.22
LLaVA-NeXT-Video	<b>35.67</b>	34.08	33.12	33.50	32.45	35.25	35.96	35.16	35.25
VideoChat	<b>51.10</b>	49.50	49.03	49.62	50.31	49.72	50.44	48.97	48.97
Video-LLaMA	<b>64.57</b>	64.11	62.98	61.99	62.08	63.56	61.94	62.17	62.89
<b>AASR</b>	<b>48.61</b>	47.69	46.76	47.07	46.44	47.67	47.42	46.74	46.83

Table 8. ASR (%) of the I2V-MLLM attack across different weight ratios of the vision model loss ( $\lambda_1$ ) and projector loss ( $\lambda_2$ ). The highest attack performance for each target model is shown in **bold**.

Target Model	Type	Correct	Detail	Context	Temporal	Consistency
Chat-UniVi	Clean	2.02	2.07	2.60	1.75	1.78
	Vanilla*	1.33 $\downarrow 0.69$	1.44 $\downarrow 0.63$	1.81 $\downarrow 0.79$	1.36 $\downarrow 0.39$	1.32 $\downarrow 0.46$
	I2V-MLLM	1.37 $\downarrow 0.65$	1.46 $\downarrow 0.61$	1.89 $\downarrow 0.71$	1.18 $\downarrow 0.57$	1.42 $\downarrow 0.36$
LLaVA-NeXT-Video	Clean	2.38	2.54	2.97	1.97	1.88
	Vanilla*	2.07 $\downarrow 0.31$	2.25 $\downarrow 0.29$	2.64 $\downarrow 0.33$	1.55 $\downarrow 0.42$	1.74 $\downarrow 0.14$
	I2V-MLLM	2.10 $\downarrow 0.28$	2.23 $\downarrow 0.31$	2.69 $\downarrow 0.28$	1.55 $\downarrow 0.42$	1.83 $\downarrow 0.05$
VideoChat	Clean	1.87	2.06	2.44	1.52	2.00
	Vanilla*	1.08 $\downarrow 0.79$	1.39 $\downarrow 0.67$	1.60 $\downarrow 0.84$	1.26 $\downarrow 0.26$	1.86 $\downarrow 0.14$
	I2V-MLLM	1.06 $\downarrow 0.81$	1.41 $\downarrow 0.65$	1.55 $\downarrow 0.89$	1.22 $\downarrow 0.30$	1.48 $\downarrow 0.52$
Video-LLaMA	Clean	1.88	1.89	2.21	1.64	1.75
	Vanilla*	1.27 $\downarrow 0.61$	1.32 $\downarrow 0.57$	1.44 $\downarrow 0.77$	1.29 $\downarrow 0.35$	1.36 $\downarrow 0.39$
	I2V-MLLM	1.26 $\downarrow 0.62$	1.33 $\downarrow 0.56$	1.42 $\downarrow 0.79$	1.34 $\downarrow 0.30$	1.25 $\downarrow 0.50$

Table 9. The results on the **ActivityNet-200** for video understanding tasks. All scores range from 1 to 5, with lower scores indicating better attack performance.  $\downarrow$  represents the performance drop compared to the clean video samples. \* indicates a white-box attack.

IMM/V-MLLMs evolves as the iteration number increases. The Pearson Correlation Coefficient (PCC) [35] is used to quantify the linear correlation between cosine similarity trends computed from both IMM and V-MLLMs. Fig. 11 presents the PCC analysis of these trends, using BLIP-2 and four different V-MLLMs. As shown, all PCC values exceed 0.90, indicating a strong positive linear relationship between the directional changes of intermediate features in IMM and V-MLLM. This suggests that perturbations in IMM’s image features can effectively disrupt the intermediate features of video samples in V-MLLMs. Notably, the PCC values between BLIP-2 and VideoChat, as well as Video-LLaMA, are exactly 1, which aligns with the highest ASR values observed for these models in Tab. 6. The slightly lower PCC values with Chat-UniVi and LLaVA-NeXT-Video correspond to the lower ASR values, demonstrating that a higher PCC between IMM and V-MLLMs indicates better adversarial transferability.

**Case study.** As shown in Fig. 12, adversarial video samples generated from the I2V-MLLM attack cause differ-

ent V-MLLMs to produce responses that differ significantly from the clean answers, demonstrating that our method effectively misleads V-MLLMs and disrupts their ability to accurately interpret the video content.

### C. Algorithm

The complete I2V-MLLM Attack process is described in Algorithm 1.

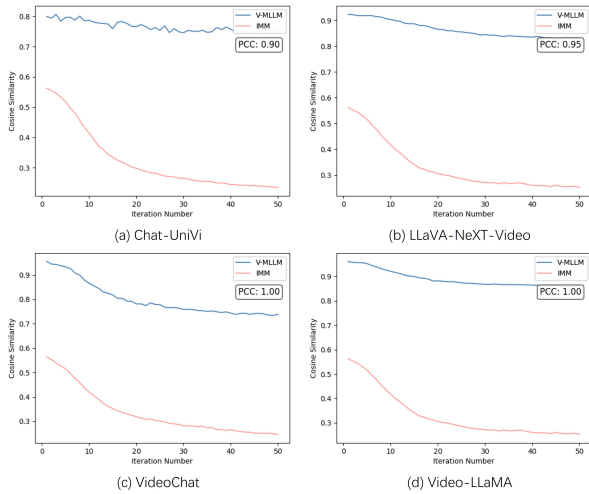


Figure 11. Pearson Correlation Coefficient (PCC) analysis between the cosine similarity trends computed from BLIP-2 and four V-MLLMs. The features of BLIP-2 are derived from vision model and projector, while the features of the V-MLLMs are obtained from the video encoders and the LLMs.

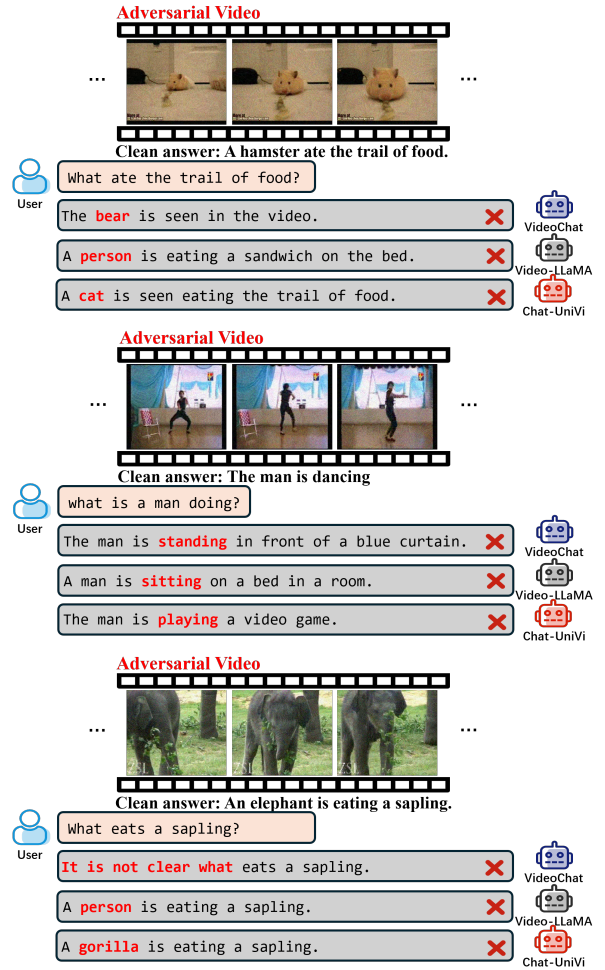


Figure 12. The adversarial video samples for VideoQA tasks are based on MSVD-QA, where the surrogate model is BLIP-2 and the target V-MLLMs are VideoChat, Video-LLaMA, and Chat-UniVi. The clean answers are the responses generated by Chat-UniVi on clean video samples. Red crosses indicate that the responses generated by V-MLLMs do not semantically align with the expected clean answers.



---

**Algorithm 1** I2V-MLLM Attack

---

**Input:** A video sample  $V$ , caption set  $T$ .

**Parameters:** Step size  $\alpha$ , iteration number  $I$ , perturbation budget  $\epsilon$ , key-frame ratio  $\beta$ , loss function weights  $\lambda_1, \lambda_2$ .

**Output:** The adversarial sample  $V_{adv}$ .

- 1: **// key-frame Selection**
  - 2: Split video  $V$  into  $K$  clips using key-frame ratio  $\beta$ , extract the first frame  $x_k$  from each clip  $v^k$ , forming key-frames  $X = \{x^1, x^2, \dots, x^K\}$
  - 3: **// Perturbation Optimization**
  - 4: Initialize  $X_{adv} = X + \delta_0, \delta_0 \in U(-\epsilon, \epsilon)$
  - 5: Get loss function  $\mathcal{L}_{total}$ .
  - 6: **for**  $i = 0, \dots, I - 1$  **do**
  - 7:   Calculate gradient for adversarial frames:
  - 8:      $g = \nabla_{X_{adv}} \mathcal{L}_{total}$
  - 9:   Update  $\delta_{i+1}$  with gradient descent:
  - 10:     $\delta_{i+1} = \delta_i - \alpha \cdot \text{sign}(g)$
  - 11:   Project  $X_{adv}$  to  $\epsilon$ -ball of  $X$ :
  - 12:     $X_{adv} = \text{clip}_{X, \epsilon}(X + \delta_{i+1})$
  - 13: **end for**
  - 14: **// Perturbation Propagation**
  - 15: **for**  $k = 1, 2, \dots, K$  **do**
  - 16:   Propagate  $\delta_I^k$  to the video clip  $v^k$ , yielding  $\delta'^k$
  - 17: **end for**
  - 18: **// Construct the adversarial video:**  
$$V_{adv} = \{v^1 + \delta'^1, v^2 + \delta'^2, \dots, v^K + \delta'^K\}$$
  - 19: **Return** the adversarial video sample  $V_{adv}$
-